CONF-970201--29

# IRRADIATION DAMAGE OF FERRITIC/MARTENSITIC STEELS: FUSION PROGRAM DATA APPLIED TO A SPALLATION NEUTRON SOURCE

R. L. Klueh
Metals and Ceramics Division
Oak Ridge National Laboratory
P.O. Box 2008, MS 6376
Oak Ridge, TN 37931-6376



## Abstract

Ferritic/martensitic steels were chosen as candidates for future fusion power plants because of their superior swelling resistance and better thermal properties than austenitic stainless steels. For the same reasons, these steels are being considered for the target structure of a spallation neutron source, where the structural materials will experience even more extreme irradiation conditions than expected in a fusion power plant first wall (i.e., high-energy neutrons that produce large amounts of displacement damage and transmutation helium). Extensive studies on the effects of neutron irradiation on the mechanical properties of ferritic/martensitic steels indicate that the major problem involves the effect of irradiation on fracture, as determined by a Charpy impact test. There are indications that helium can affect the impact behavior. Even more helium will be produced in a spallation neutron target material than in the first wall of a fusion power plant, making helium effects a prime concern for both applications.

## Introduction

The first structural materials proposed for fusion reactors were austenitic stainless steels. For higher operating temperatures (≥700°C), superalloys and refractory metal (Nb, Mo, V, and Ti) alloys were considered. Ferritic/martensitic steels were first suggested in the late 1970s [1,2]. As a result of work during the last fifteen years or so, most of the refractory metal alloys and superalloys have been eliminated. Austenitic stainless steels are concluded to be unsuitable for high heat flux applications in a fusion power plant because of high thermal stresses caused by low thermal conductivity and high thermal expansion, although they are still being considered for near-term experimental fusion machines, such as the International Thermonuclear Experimental Reactor (ITER).

Conventional martensitic steels have elevated-temperature strength and thermal properties (conductivity and expansion coefficient) that result in excellent resistance to thermal stresses [1,2]. Creep strength is adequate to 550-600°C, and the steels have been used at these temperatures in the power-generation and chemical and petrochemical industries. Because of the widespread use for such industrial applications, the technology for production and fabrication of all types of product forms exists. Likewise, the metallurgical characteristics and mechanical and physical properties are well understood, and comprehensive mechanical properties compilations are available. Uncertainties in their application involve the effects of neutron irradiation.

Most of the irradiation-effects information on ferritic/martensitic steels for fusion applications comes from studies on commercial Cr-Mo steels with 9-12% Cr, 1-1.5 % Mo, 0.1-0.2 %C (all compositions are in wt %) with small amounts of V, Nb, Ni, W, etc. These were the first ferritic steels considered for fusion applications in Japan, Europe, and the United States [2] because they had been studied for the fast breeder reactor program, where they were found to be swelling resistant compared to austenitic stainless steels, which were then considered the primary candidate material. Recently, these fusion materials programs have been developing steels that would lessen the environmental impact of fusion. Such "reduced-activation" steels display the same general behavior as conventional steels. Details on the development of these reduced-activation steels have been published [3-6]. For the purposes of this discussion, it will be enough to state that the reduced-activation steels were patterned after the conventional Cr-Mo steels, such as 9Cr-1MoVNb and 12Cr-1MoVW, but with the molybdenum replaced by tungsten and niobium replaced by tantalum [3].

From the wealth of data available, indications are that a range of conventional and reduced-activation ferritic/martensitic steels have properties that make them viable candidates for fusion applications to ≈600°C. The maximum operating temperature will be determined by creep properties and, under some circumstances, by compatibility with the operating media (i.e., water, liquid lithium, liquid Pb-Li eutectic, etc.) of the fusion power plant. The major difference in the fusion environment and in fast or thermal fission reactors is the high-energy neutron flux produced by the 14MeV neutrons from the fusion reaction.

Radiation damage occurs when high-energy neutrons displace atoms of the steel from their normal lattice positions into interstitial positions to form "interstitials" and "vacancies" (vacant lattice sites) [7]. It is the disposition of the interstitials and vacancies that determines the effect of the irradiation on the properties. Such displacement damage is the source of property changes caused by irradiation in a fast fission reactor, such as the Fast Flux Test Facility (FFTF) or the Experimental Breeder Reactor (EBR-II). However, in addition to the displacement damage, the higher-energy spectrum (up to 14 MeV) in a fusion reactor will produce large amounts of transmutation helium in the first wall and blanket structure. The effect of the simultaneous formation of displacement damage and transmutation helium on properties must be determined. Other transmutation products are formed, including hydrogen and other metal atoms. However, the hydrogen is expected to diffuse from the steel at reactor temperatures, and small amounts of other metals are not expected to affect the properties.

Structural materials in the target of a spallation neutron source will experience neutron irradiation effects similar to or greater than those in the first wall of a fusion power plant because of the presence of higher neutron energies (to 200 MeV and above) that will create even higher helium concentrations. Typically, the He/dpa ratios in fission, fusion, and spallation neutron sources are estimated to be about 1, 10, and 100, respectively. It is of interest to examine the irradiation behavior of the ferritic/martensitic steels as determined for fusion to anticipate the effects expected in the spallation neutron source application.

## Materials and Experimental Procedures

### Test Materials

This discussion will refer mainly to the materials studied in the U.S. Fusion Materials Program, although similar materials have been studied in Europe and Japan [2]. The primary commercial ferritic/martensitic steels considered in the U.S. program were Sandvik HT9 (nominally Fe-12Cr-1Mo-0.25V-0.5W-0.5Ni-0.2C, here designated 12Cr-1MoVW) and modified 9Cr-1Mo steel (nominally Fe-9Cr-1Mo-0.2V-0.06Nb-0.1C, designated 9Cr-1MoVNb) [8].

HH

## DISCLAIMER

## DISCLAIMER

Portions of this document may be illegible in electronic image products. Images are produced from the best available original document.

The reduced-activation steels are similar to the commercial steels but with the molybdenum replaced by tungsten and the niobium by tantalum. One such steel will be discussed here; it was developed at the Oak Ridge National Laboratory (ORNL) [9] with the nominal composition of Fe-9Cr-2W-0.25V-0.07Ta-0.1C and is designated as 9Cr-2WVTa.

Miniature tensile (44.5 or 25.4 mm long with gage section dimensions of 20.3 x 1.52 x 0.76 mm or 7.62 x 1.52 x 0.76 mm, respectively) and miniature Charpy (⅓ size: 3.3 x 3.3 x 25.4 mm, or ½ -size: 5 x 5 x 25.4mm) specimens were machined from the steels in the normalized-and-tempered condition. The steels were normalized by austenitizing at 1050°C and then rapidly cooling in air or an inert gas. Tempering was 1 h at 760°C for the 9Cr-1MoVNb steel, 2.5 h at 780°C for the 12Cr-1MoVW steel, and 1 h at 750°C for the 9Cr-2WVTa steel. The microstructure after this heat treatment is tempered martensite.

Details on the chemical compositions, heat treatments, microstructures, and test procedures have been published [8,9].

Neutron Irradiation Studies

One difficulty in developing materials for fusion is that no fusion reactor is available to test materials. Therefore, the expected neutron irradiation effects must be simulated, primarily by irradiation in fission reactors. Displacement damage in fusion and fast fission reactors is similar, and fast reactors, such as the FFTF and the EBR-II, have been used to study displacement damage, although neutrons with much higher energy (up to 14 MeV) are produced by the fusion reaction than in a fast fission reactor (average neutron creation energy in a fast reactor is ≈2MeV). The higher-energy neutrons will produce more transmutation helium in a material than produced by fast-fission irradiation. The simultaneous development of displacement damage and helium in a fusion power plant could affect both the swelling behavior and the mechanical properties relative to the formation of displacement damage alone. Therefore simulation techniques are required to study helium effects.

Helium effects in martensitic steels can be simulated by irradiating a steel containing nickel in its composition or one to which a small amount of nickel has been added in a mixed-spectrum reactor, such as the High Flux Isotope Reactor (HFIR) [8],where both fast and thermal neutrons are generated. Thermal neutrons react with $^{58}Ni$ to produce helium by the two-step reaction $^{58}Ni(n,\gamma)^{59}Ni(n,\alpha)^{56}Fe$. Therefore, displacement damage is produced by the fast neutrons simultaneously with the production of transmutation helium by the thermal neutrons. For a steel containing 2% Ni irradiated in the HFIR, the same amount of helium (in appm) per atom displaced (He/dpa ratio) forms as is expected to form in a Tokamak fusion power plant [8].

Results and Discussion

Swelling Behavior

As discussed above, it is the disposition of the interstitials, vacancies, and transmutation helium created by irradiation that determines the effect of the irradiation on mechanical and physical properties. At reactor temperatures, interstitials and vacancies are mobile, and most are eliminated by a one-to-one recombination and therefore have no effect on properties. Many of those that do not recombine migrate to "sinks," where they are absorbed. Sinks include surfaces, grain boundaries, dislocations, and existing cavities. The remainder form clusters of self defects or defects and impurity atoms. Mechanical and physical properties are affected by the defect clusters. Clusters consisting of interstitials can evolve into dislocation loops, and vacancy clusters can develop into microvoids or cavities. Solute clusters can also form under certain conditions. Vacancies become increasingly mobile above 0.3 $T_m$, where $T_m$ is the absolute melting temperature, and a dislocation and cavity structure results to produce void swelling. This microstructure, which is accompanied by an increase in volume (swelling), occurs because interstitials are accepted preferentially by dislocations. This leaves an excess of vacancies to be absorbed by cavities, giving rise to the observed swelling. Cavities are stabilized by helium, which is a strong cavity nucleation agent.

Ferritic steels were first considered for fusion because of the swelling resistance displayed in fast reactor irradiations. They have the best swelling resistance of all fusion candidate materials. This is demonstrated in Fig. 1, where the behavior of several heats of commercial ferritic steels are compared to type 316 stainless steel after irradiation at 420°C to ≈80 dpa [10]. Even after irradiation to 200 dpa near the peak swelling temperature of 420°C in the FFTF, total swelling of only 0.09 and 1.02% was measured for 12Cr-1MoVW in two different heat treatment conditions, and 1.76% for 9Cr-1MoVNb steel [11]. Steady state swelling rates for the 9Cr-1MoVNb and 12Cr-1MoVW steels have been estimated at ≈0.015%/dpa, compared with 1%/dpa for a type 316 stainless steel [12]. Similar low swelling rates have been observed for reduced-activation steels irradiated to 200 dpa [13]. Helium concentrations have been shown to increase swelling rates, but even when the steel contains several-hundred appm He, swelling rates remain low [14].

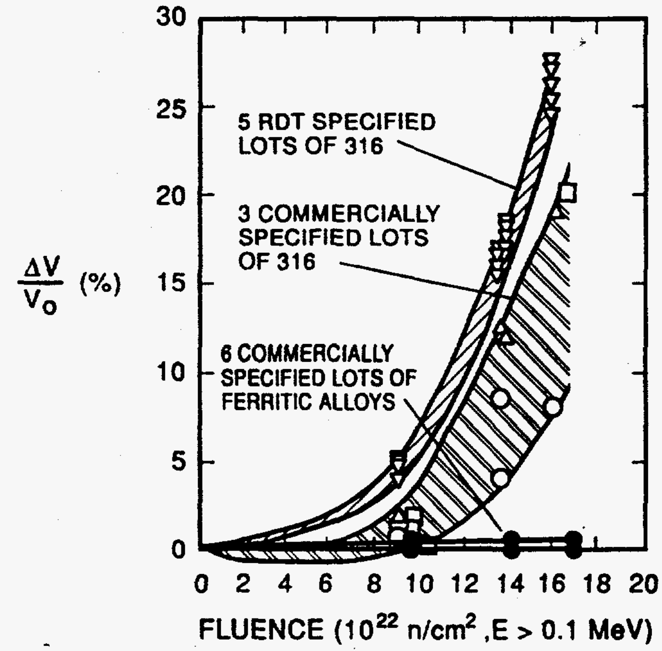


Figure 1: Swelling behavior of six commercial heats of ferritic/martensitic steels compared to type 316 stainless steel after irradiation in EBR-II at 420°C to ≈80 dpa. After Gelles [10].

Irradiation Hardening

Irradiation in a fast reactor such as EBR-II or FFTF results in displacement damage with little helium formation. Irradiation temperatures are controlled by the sodium coolant temperature, and irradiations can be carried out between about 360 to 700°C. An example of the effect of fast-reactor irradiation on the 0.2% yield stress (YS) and ultimate tensile strength (UTS) of 9Cr-1MoVNb steel is shown in Fig. 2 [15]. Irradiation was at 390, 450, 500, and 550°C in EBR-II to ≈9 dpa with tensile testing at the approximate irradiation temperature. Also shown are data for unirradiated normalized-and-tempered specimens and for unirradiated specimens thermally aged at the irradiation temperature for 5000 h, the approximate time in reactor.

Thermal aging had little or no effect at all temperatures. Considerable irradiation hardening occurred at 390°C as observed by large increases in both the YS and the UTS [Fig. 2(a)]. At 450, 500, and 550°C, irradiation caused little or no change in YS or UTS [15]. The effect of irradiation on ductility reflected the effect on strength [Fig. 2(b)] [15]. Uniform and total elongation at 390°C were less than those of the unaged and aged controls, with essentially no change occurring at the three highest irradiation temperatures [15].

Specimens of 12Cr-1MoVW (HT9) steel were irradiated to 13 dpa in the same experiment as the 9Cr-1MoVNb steel [16]. Similar effects were observed: irradiation hardening occurred at 390°C, and essentially no change in properties occurred from irradiation at 450, 500, and 550°C. Both the 9Cr-1MoVNb and 12Cr-1MoVW steels were further irradiated in EBR-II to 23 to 25 dpa at the same temperatures [17]. At 390°C there was little change relative to the steels irradiated to 9 to 13 dpa, an indication that the hardening saturated at or before a fluence of 9 dpa was reached. After irradiation at 450,

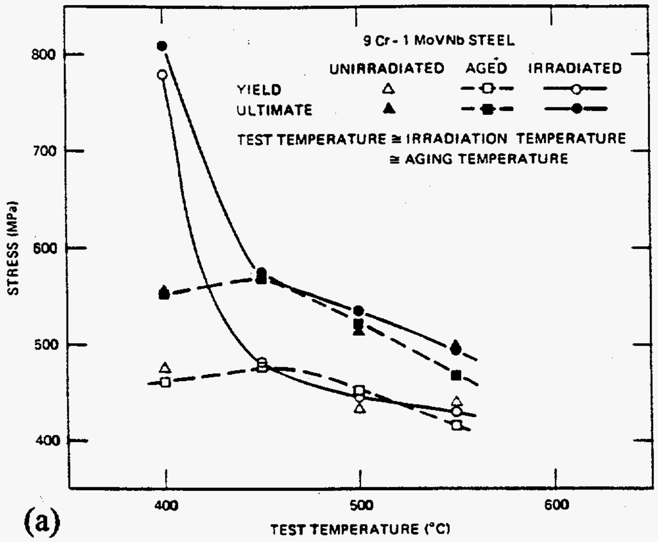


(a)

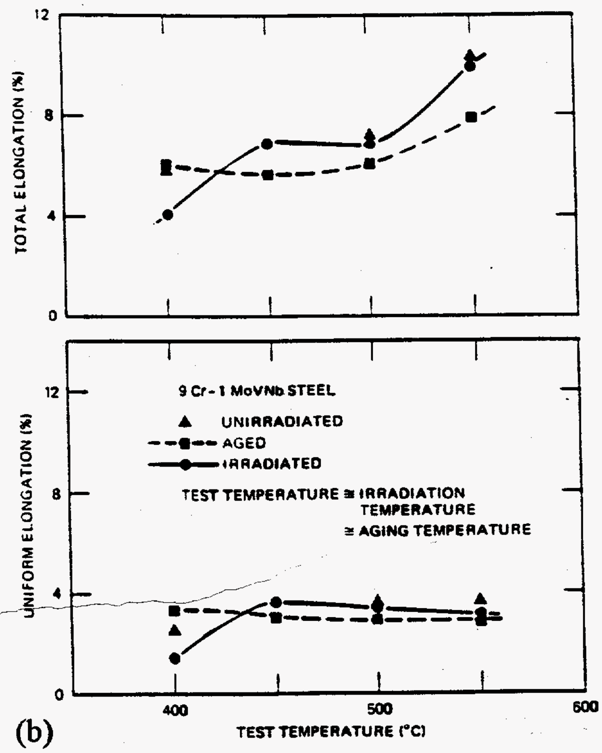


(b)

Figure 2: (a) Yield stress and ultimate tensile strength and (b) uniform and total elongation of normalized-and-tempered, thermally aged, and irradiated 9Cr-1MoVNb steel.

500, and 550°C, there was again little difference in the tensile properties of the irradiated and the unirradiated specimens [17].

Transmutation helium can affect the behavior of an irradiated alloy in three ways [18]. First, helium can stabilize vacancy clusters, which, in turn, can cause an increase in the number of interstitial clusters (i.e., helium ties up vacancies and reduces interstitial-vacancy recombination). Interstitial clusters can then grow into dislocation loops and increase the strength; vacancy clusters can also affect strength under some conditions. Secondly, helium stabilizes the clusters to a higher temperature than in the absence of helium. The third effect involves the migration of helium to grain boundaries during irradiation, which can then affect mechanical properties, especially the ductility.

To determine the effect of the simultaneous formation of displacement damage and transmutation helium on tensile behavior, the 9Cr-1MoVNb and 12Cr-1MoVW steels and these two steels with up to 2% Ni were irradiated in HFIR at 50, 300, 400, 500, and 600°C [19-21]. The results at 400-600°C were compared with the same steels irradiated in EBR-II, where very little helium formed [21]. The experiments indicated that there was probably a small hardening effect superimposed on the hardening due to displacement damage alone [19,20]. However, because of the scatter in the results, different conditions in the different experiments, and because the temperature range around 400°C is where the least hardening is expected, it was difficult to determine the magnitude of that effect. It was concluded that the effect is probably not large in relation to the hardening caused by displacement damage alone.

Elevated-Temperature Helium Embrittlement

For irradiation temperatures above 425-450°C, displacement damage is unstable, and flow properties are essentially unaffected by irradiation. However, in certain alloys that contain helium, the ductility after irradiation decreases in tensile or creep tests at >600°C because of elevated-temperature helium embrittlement [7]. Intergranular fracture occurs, and the loss of ductility is caused by helium on grain boundaries [7]. For the austenitic stainless steels, the ductility can be reduced to much less than 0.1% with the presence of only a few appm He—even the small amounts formed during fast-reactor irradiation [7]. Several investigators have examined the effects in ferritic steels at 500-700°C and have concluded that these steels are relatively immune to the effect, at least for helium levels up to a few-hundred appm [22-24].

Irradiation Embrittlement

A major concern for ferritic/martensitic steels irradiated in light-water reactors, fast reactors, and fusion power plants is the effect of irradiation on low-temperature (≤400-425°C) impact toughness, as measured in a Charpy V-notch test as an increase in the ductile-brittle transition temperature (DBTT) and a decrease in the upper-shelf energy (USE) [25]. Even if the DBTT is below room temperature before irradiation, it can be well above room temperature after irradiation. Irradiation embrittlement is related to hardening caused by the radiation-produced dislocation loops that form below ≈0.3 $T_m$ (<425-450°C in the ferritic/martensitic steels); hardening increases with decreasing irradiation temperature. Irradiation-induced precipitates can also have an effect. Irradiation increases the flow stress, and under the assumptions that the fracture stress is unaffected by irradiation and that the intersection of the fracture stress curve and the flow stress curve is the DBTT for the unflawed condition, the increase in flow stress by irradiation causes a shift in the DBTT (shown schematically in Fig. 3) [25].

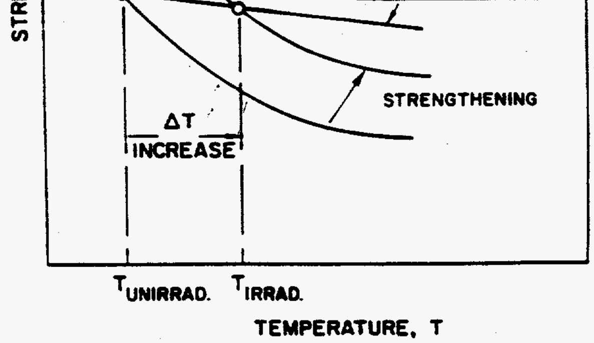


Figure 3: Schematic diagram that illustrates how strength increase due to irradiation causes a shift in the ductile-brittle-transition temperature.

A shift in DBTT (ΔDBTT) of ≈160°C was observed when the 12Cr-1MoVW steel was irradiated to 10 dpa at 365°C in FFTF (Fig. 4) [26]. Irradiation to 17 dpa gave a similar shift, indicating that a saturation with fluence occurred (Fig. 4), just as saturation occurred for hardening in a tensile test [17]. Although the Charpy curves for the steels are shifted by irradiation, the fracture mode is unaltered between the irradiated and unirradiated steels, with cleavage-type failure occurring on the lower shelf and ductile void coalescence occurring on the upper shelf.

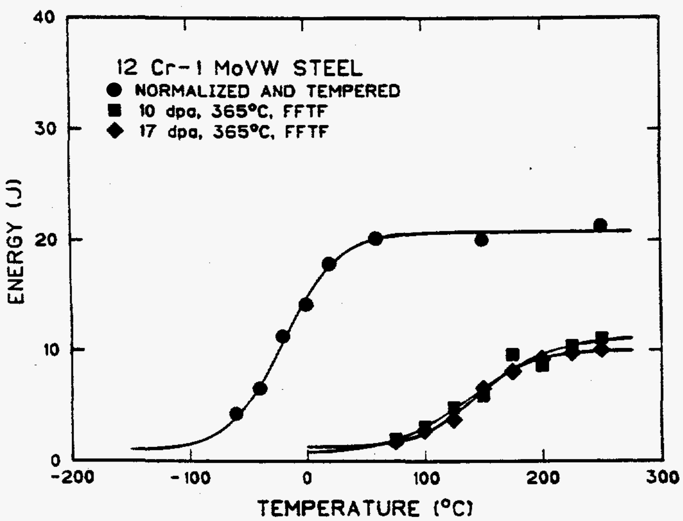


Figure 4: Charpy curves for half-size specimens of 12Cr-1MoVW steel before and after irradiation to 10 and 17 dpa at 365°C in FFTF.

Most irradiation studies have been in fast reactors at temperatures between 365 and 600°C (lower temperatures are generally not possible in fast reactors ). Hu and Gelles [27] irradiated 9Cr-1MoVNb and 12Cr-1MoVW steels at 390, 450, 500, and 550°C in EBR-II to 13 and 26 dpa (Fig. 5). For the 9Cr-1MoVNb steel irradiated at 390°C, the ΔDBTT saturated by 13 dpa (values of 52 and 54°C were obtained after 13 and 26 dpa, respectively). Irradiation of the 9Cr-1MoVNb steel in EBR-II at 450, 500, and 550°C resulted in little change in the DBTT, in agreement with the observation that hardening vanishes above 425-450°C [Fig. 2(a)].

It has also been concluded that saturation occurred for the 12Cr-1MoVW steel irradiated by Hu and Gelles at 390°C, although values of 124 and 144°C were obtained after 13 and 26 dpa, respectively (Fig. 5) [27]. Also, as seen in Fig. 5, it is apparent that the ΔDBTT did not go to zero at 450, 500, and 550°C for 12Cr-1MoVW steel, as observed for the 9Cr-1MoVNb steel, even though there was no hardening for the 12Cr-1MoVW above 400°C [16]. The reason for this can be found in the microstructures of the two steels. The 12Cr-1MoVW contains twice as much carbon as the 9Cr-1MoVNb steel (0.2% vs. 0.1%), and in the normalized-and-tempered condition, the 12Cr-1MoVW contains over twice as much precipitate (3.8 wt% precipitate in the 12Cr-1MoVW compared to 1.5 wt% in 9Cr-1MoVNb) [28]. The majority of the precipitate in both steels is $M_{23}C_6$, with a small amount of MC [28]. A larger amount of large $M_{23}C_6$ precipitates was relatively uniformly distributed in the 12Cr-1MoVW steel [28]. Fracture in steels is generally initiated at carbide particles or inclusions [29,30]. The difference in precipitates can affect the fracture process because the larger precipitate particles can result in a larger initial crack size. The fact that the ΔDBTT did not go to zero at 450-550°C even though hardening did not occur in 12Cr-1MoVW at these temperatures [16,17] can also be attributed to the large precipitates, which could grow larger by irradiation-enhanced diffusion during irradiation at the higher temperatures.

The ORNL 9Cr-2WVTa reduced-activation steel was also irradiated at 365°C in FFTF, and it showed exceptionally small shifts in DBTT: 4, 14, 21, and 32°C after 6.4, 15.4, 22.5, and 28 dpa, respectively [9]. This compares with the 12Cr-1MoVW irradiated at 365°C in FFTF that saturated at or below 10 dpa after a shift of ≈160°C (Fig. 4) [26]. Not only does the 9Cr-2WVTa show a very small ΔDBTT (32°C), but because it has a very low DBTT in the unirradiated condition (-88°C), the DBTT after irradiation is considerably below

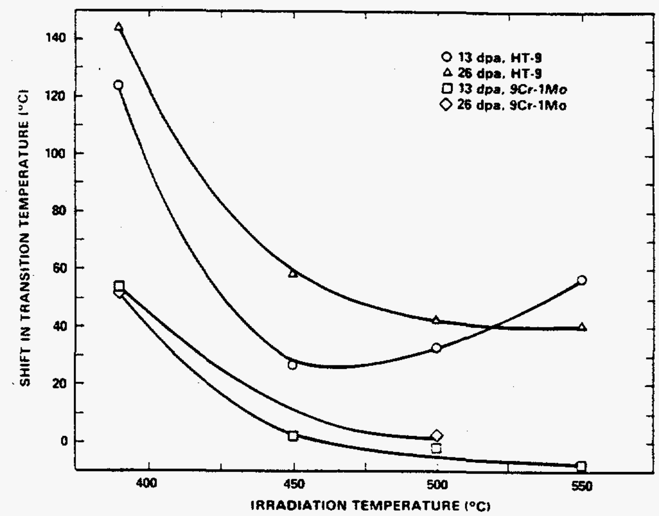


Fig. 5: Variation of the shift in DBTT with temperature and fluence. After Hu and Gelles [27].

that for any other steel after irradiation. This is demonstrated in Fig. 6, where the 9Cr-2WVTa is compared with the 12Cr-1MoVW before and after irradiation in FFTF at 365°C. The DBTT for the 9Cr-2WVTa after irradiation is lower (-56°C) than for any of the other steels (9Cr-1MoVNb, 12Cr-1MoVW, and other reduced-activation steels) before irradiation. Figure 6 is a comparison of the steel (12Cr-1MoVW) that was the first ferritic/martensitic steel candidate in the U.S. Fusion Materials Program with one of latest experimental steels and indicates the progress that has been achieved in developing steels for radiation resistance.

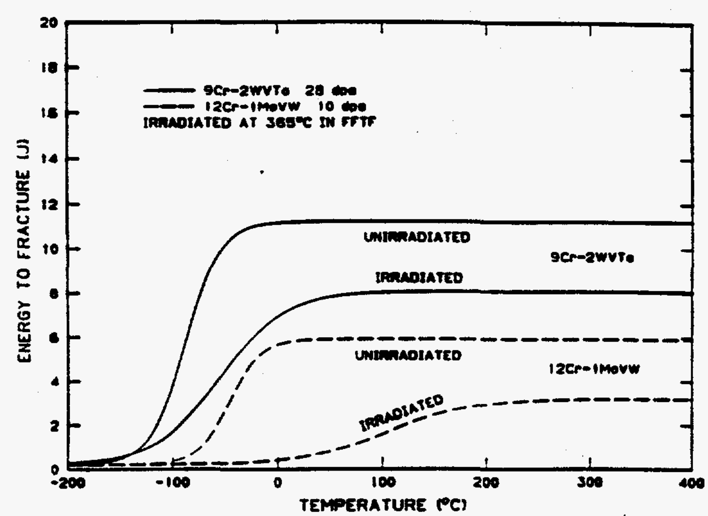


Figure 6: Comparison of the unirradiated and irradiated Charpy curves for third-size specimens of 12Cr-1MoVW and 9Cr-2WVTa steels.

The exceptional behavior of the 9Cr-2WVTa steel was further demonstrated by Rieth and co-workers [31] who irradiated the steel with several reduced-activation steels (F82H, OPTIFER I and OPTIFER II) and conventional Cr-Mo steels (MANET I and II) in the HFR reactor at 250-400°C to 0.8 dpa (Fig. 7). The 9Cr-2WVTa steel (labeled ORNL in Fig. 7) has the lowest DBTT [31]. This superior behavior has now been shown to continue out to 2.5 dpa [32].

The nickel-doping technique was used to study the effect of helium on the Charpy properties of 9Cr-1MoVNb and 12Cr-1MoVW steels [33-36]. Charpy specimens of the following five steels were irradiated in the HFIR (a mixed-

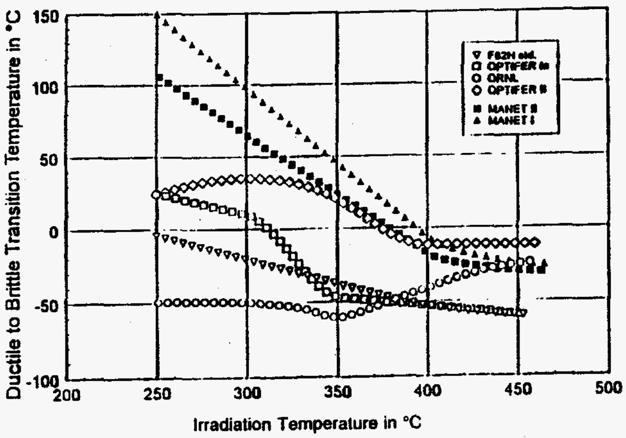


Figure 7: DBTT as a function of temperature for four reduced-activation and two conventional martensitic steels irradiated to 0.8 dpa in the HFR.

spectrum reactor): 9Cr-1MoVNb, 12Cr-1MoVW, 9Cr-1MoVNb-2Ni (standard 9Cr-1MoVNb with 2% Ni), 12Cr-1MoVW-1Ni, (standard 12Cr-1MoVW with 1% Ni), and 12Cr-1MoVW-2Ni (standard 12Cr-1MoVW with 2% Ni). The compositions of standard 9Cr-1MoVNb and 12Cr-1MoVW steels contain ≈0.1 and ≈0.5% Ni, respectively,

Results from HFIR irradiation, where helium was generated, were compared with results from irradiations of these steels in the EBR-II, a fast reactor where little helium forms [33-36] (Fig. 8). In irradiations to 13 and 26 dpa at 390°C in EBR-II, Hu and Gelles [27] found that the ΔDBTT saturated with fluence at ≈54°C for 9Cr-1MoVNb and ≈144°C for 12Cr-1MoVW; the ΔDBTT saturated by or before 13 dpa. Other fast-reactor irradiations demonstrated that saturation occurs by 10 dpa or less [26]. Corwin, Vitek, and Klueh [35] irradiated the same heats of 12Cr-1MoVW and 12Cr-1MoVW-2Ni steels used in the HFIR experiments to 12 dpa in EBR-II at 390°C and found shifts in DBTT of 90 and 122°C, respectively, in line with the Hu and Gelles data for 12Cr-1MoVW [27].

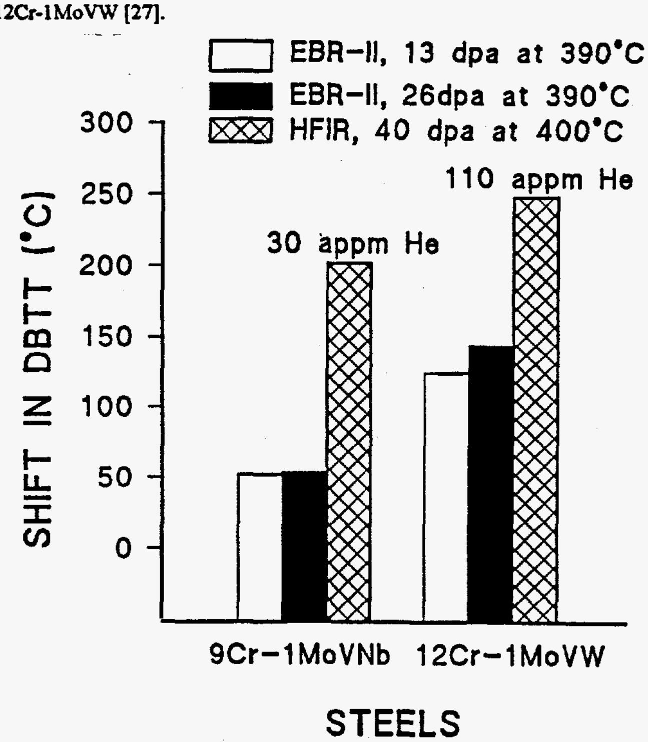


Figure 8: A comparison of the shift in DBTT after irradiation in EBR-II to 13 and 26 dpa and in HFIR to 40 dpa for 9Cr-1MoVNb and 12Cr-1MoVW steels.

The ΔDBTT for the 9Cr-1MoVNb (204°C) and the 12Cr-1MoVW (242°C) steels after irradiation in HFIR at 400°C to ≈40 dpa [33] were considerably above the values observed after irradiation in EBR-II to 13 and 26 dpa (Fig. 7) [27,35]. After irradiation in HFIR, the 9Cr-1MoVNb contained 32 appm He, and the 12Cr-1MoVW contained 105 appm He, attributed to nickel contents of the steels of 0.1 and 0.5%, respectively. The difference in properties was taken to indicate that the saturation in ΔDBTT observed in the EBR-II at 390°C did not apply to irradiation in the HFIR. Further, when the 12Cr-1MoVW-2Ni and 9Cr-1MoVNb-2Ni were irradiated in HFIR at 400°C to ≈40 dpa and ≈370 appm He, the ΔDBTTs were >325°C, which was considerably above the values observed for the steels without the nickel additions and was taken as further evidence of a helium effect [33]. Examination of some of the fractured specimens provided some indication of intergranular fracture [33]. Irradiation at 300°C showed that there was an effect of helium when the steels with 2% Ni were compared with those to which no nickel had been added [33]. However, the ΔDBTT at 300°C for the respective steels with and without the nickel additions was considerably less than at 400°C, which is opposite to the temperature effect observed for the steels irradiated in a fast reactor over the range 365-550°C (i.e., the ΔDBTT decreases with increasing irradiation temperature for irradiation in a fast reactor) (Fig. 5) [27,35].

After considering possible explanations for the difference in ΔDBTT for the same steels irradiated in HFIR and EBR-II and why steels with 2% Ni are more brittle than those with less nickel when irradiated in HFIR, it was concluded that helium plays a role [33]. This helium effect is in addition to the effect caused by the irradiation hardening from dislocation loops and irradiation-enhanced precipitation [33,34]. Since excess hardening by helium (above that from dislocation loops and precipitation) as measured in tensile tests could not explain the observation, it was suggested that helium causes a decrease in fracture stress (the third helium effect discussed in the previous section). From a limited number of observations of intergranular fracture, it was concluded that helium promotes intergranular fracture, which was interpreted to mean that there was a decrease in the fracture stress (see Fig. 3) [33,34].

An increase in DBTT can be caused by: (1) more or larger flaws, (2) less resistance to the initiation of a flaw, and (3) less resistance to the propagation of a flaw. Inclusions or carbides are likely sources of microcracks that initiate fracture in steels [29,30]. The larger ΔDBTT for 12Cr-1MoVW than 9Cr-1MoVNb in FFTF (little helium) was attributed to the larger amounts of large precipitate particles in the 12Cr-1MoVW steel [33,34]. The 12Cr-1MoVW contains twice as much precipitate as 9Cr-1MoVNb because it contains twice as much carbon [33,34].

To explain the helium effect, it was proposed that when the steels contain sufficient helium, the microcrack source could be helium bubbles on a prior-austenite grain boundary or a lath boundary [33,34]. Helium is envisioned to collect into small cavities that under stress become nuclei for fracture and/or enhance crack propagation, explaining why fracture surfaces of HFIR-irradiated, helium-containing steels contain intergranular facets. This hypothesis can explain the reverse temperature effect (a larger shift at 400°C than 300°C) relative to fast-reactor irradiations. More rapid diffusion of helium at 400°C than at 300°C means that at 400°C more helium reaches boundaries to produce more and larger bubbles and a larger ΔDBTT. Bubble development at 300°C is slower than at 400°C, but it will be increased by higher fluences (longer diffusion times) or higher helium generation rates, with a corresponding increase in the ΔDBTT. This was observed for the 9Cr-1MoVNb-2Ni and 12Cr-1MoVW-2Ni irradiated to 27 dpa at 300°C, where these steels developed a larger ΔDBTT than the steels without any nickel additions [30].

Figure 9 shows the data for the ΔDBTT-temperature relationship for the 9Cr-1MoVNb steel with a schematic representation of how the various irradiation effects are postulated to affect fracture behavior between 50 and 550°C [34]. Between 400 and 550°C, the only data available are those from EBR-II [27]. Although no data are available for irradiation in fast reactors below ≈365°C, a postulated curve for EBR-II irradiation down to 50°C is shown. Irradiation-produced defects and precipitates account for the DBTT shift after irradiation in EBR-II. The relative contribution of the two processes is temperature dependent, with precipitation becoming more important with increasing temperature, but with the effect of both hardening processes becoming negligible above ≈450°C [34]. Irradiation in HFIR was postulated to lead to a further increment of hardening caused by helium [19-21], which the tensile

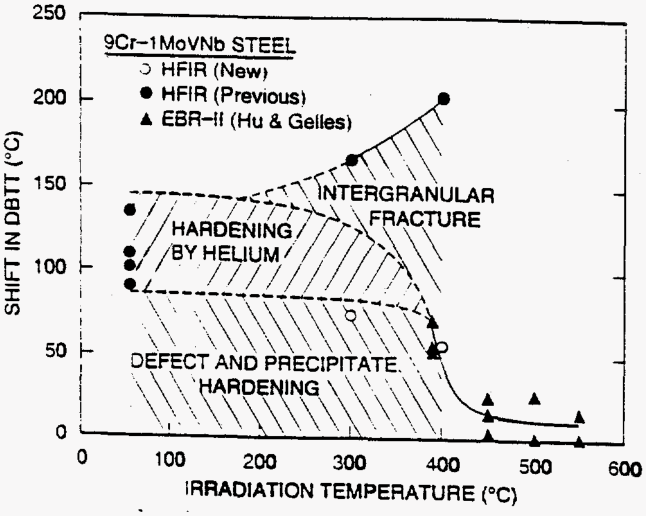


Figure 9: A graphical representation of the shift in DBTT as a function of irradiation temperature for 9Cr-1MoVNb steel to indicate the postulated hardening and fracture mechanisms.

behavior indicated also decreases to zero above 425-450°C [20,21]. As discussed above, the degree of hardening due to helium is probably not large and has not been adequately assessed, making the extent of this region uncertain. In this helium-affected region and the region where hardening is dominated by defects and precipitates, the brittle region of the Charpy curve is characterized by cleavage and/or quasi-cleavage. Around 300°C up to 400°C, intergranular fracture in the presence of helium becomes important. The shape of the intergranular-fracture portion of the diagram will depend on the helium concentration, temperature, and fluence. For application of ferritic steels in spallation neutron sources where helium generation rates are ten times higher than for fusion reactors, this is the region that demands greater attention.

Similar reasoning applies for the 12Cr-1MoVW steel, although a diagram for this steel will be complicated by the increase in the ΔDBTT with increasing temperature, because of the effect precipitation on fracture mode [34]. It should be noted that the 50°C tests for both steels were for relatively low-fluence irradiations (<10 dpa), and therefore, saturation may or may not have been achieved [36]. The low-temperature irradiations also showed a slightly higher ΔDBTT for the nickel-doped steels [36], in agreement with the small hardening effect of helium observed in tensile tests of the steels irradiated at 50°C [19].

If helium plays the role postulated in the previous section, then, depending on the operating temperature, the impact toughness could be affected in the target structure of a spallation neutron source, where large amounts of helium would be generated. With enough helium, the ΔDBTT at 300°C would be expected to increase. Since the helium effect postulated above depends on diffusion, it is unclear how low in temperature the helium could affect impact properties by the postulated mechanism. It is also unclear what might happen above 400°C, since no HFIR experiments were conducted at these temperatures. The diffusion rate increases with temperature, thus increasing the rate at which helium can migrate to boundaries. On the other hand, irradiation hardening decreases rapidly above 400°C and disappears above ≈425-450°C [15-17]. If hardening is needed for this embrittlement, then even if helium is present on boundaries, the reduced yield stress would probably preclude a larger ΔDBTT than observed for fast reactor irradiation. (This embrittlement is different from elevated-temperature embrittlement, where hardening is not required. As stated above, the ferritic steels appear immune to elevated-temperature helium embrittlement up to few-hundred appm He. The effect of the levels of large helium concentrations expected in spallation neutron sources has not been examined.)

A target structure design for a spallation source would be such as to keep the operating temperature above the DBTT. Figure 9 indicates that 9Cr-1MoVNb could then probably be used above 400-450°C. It may also be possible to use the steel below some temperature, say ≈200-250°C, where diffusion of helium would not allow the postulated embrittlement mechanism to operate. If such low-temperature operation is possible, then a steel such as the 9Cr-2WVTa would provide a larger safety margin because it has such a low DBTT before and after irradiation in a fast reactor.

To minimize the effect of helium in austenitic stainless steels, microstructures were developed with a high number density of fine precipitates [37]. For such a microstructure, the transmutation helium formed during irradiation is trapped at the matrix/precipitate interfaces. Because of the large number of precipitates, the helium is widely distributed, and the high number density of small bubbles that form (as opposed to a smaller number of large bubbles) suppress swelling. Elevated-temperature helium embrittlement, which causes low-ductility fractures in irradiated austenitic stainless steel containing helium tested in tension or creep, is also inhibited because the precipitates prevent helium from migrating to grain boundaries [37]. A similar process might be effective in the ferritic steels to minimize the effect of helium on the shift in DBTT.

The 9Cr-2WVTa, like other 9-12% Cr steels, has a low number density of precipitates, which are mainly relatively large $M_{23}C_6$ particles, with a lesser number of smaller MC particles [Fig. 10(a)] [38]. Low-chromium Cr-W steels

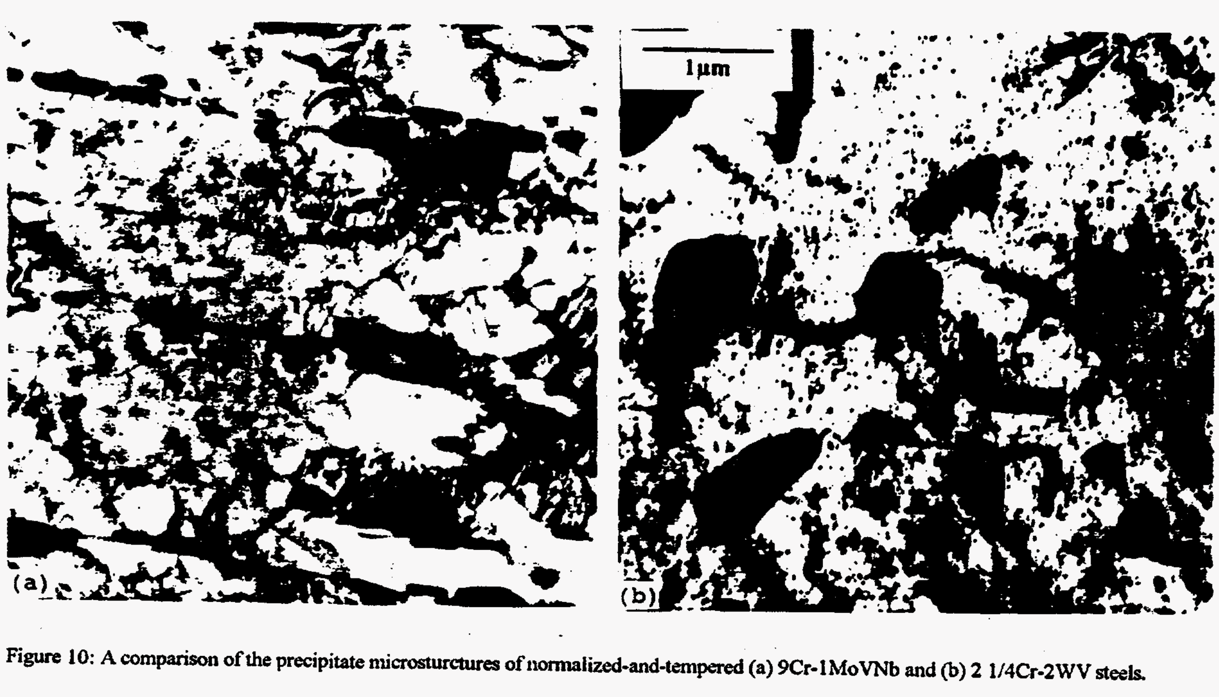


Figure 10: A comparison of the precipitate microsturctures of normalized-and-tempered (a) 9Cr-1MoVNb and (b) 2 1/4Cr-2WV steels.

can develop a higher number density of fine precipitates particles, as shown in Fig. 10(b) for a 2 1/4Cr-2WV steel [38]. The fine precipitates in 2 1/4Cr-2WV consist mainly of vanadium-rich MC [38]. The $M_{23}C_6$ and MC precipitates in 9Cr-2WVTa are present in similar number density to those in 9Cr-1MoVNb and 12Cr-1MoVW, which showed the effects of helium on properties when irradiated in HFIR [33-36]. The $M_{23}C_6$ precipitates are generally large and of low number density. MC particles are present in the high-chromium steels, but in much lesser amounts than the $M_{23}C_6$. The number of precipitates in these steels is too small to effectively trap the helium during irradiation. Figure 10(b) indicates that it may be possible to develop a high density of precipitates in a low-chromium steel. Of course, to be successful it will also be necessary to develop a steel with improved impact toughness in the unirradiated condition over that for 2 1/4Cr-2WV [38]. Such steels are being developed. A 3Cr-3WV steel has been shown to have a DBTT below that of the 9Cr-2WVTa [39]. Unfortunately, no information is available on the effect of irradiation on these steels.

It should be pointed out that the use of Charpy tests to evaluate embrittlement has limited applicability. A critical need exists for fracture toughness data, and an understanding of how the Charpy data are related to fracture toughness needs to be developed. Only with such data can the implications of the helium effects be evaluated in the proper context. Finally, it needs to be pointed out that the nickel-doping technique is not the ideal method for studying the helium effect, and a high-energy neutron source is required to verify that the observations are due to helium. Alternate explanations for the HFIR observations were considered [33,34], including the effect of other transmutation reactions with thermal neutrons in HFIR, thermal aging effects, and nickel involvement in the hardening effects. However, none of these provided a satisfactory explanation for the observations [33,34].

## Summary and Conclusions

Neutron irradiation effects on the mechanical properties of the ferritic/martensitic steels have been investigated to determine the applicability of the steels for fusion applications. Because of the similarity in the expected irradiation environment of a spallation neutron source target and the first wall of a fusion power plant, the fusion studies can be used to demonstrate some of the radiation effects to be expected for a spallation neutron source. The major problem for the steels is the effect of irradiation on impact toughness, as measured in a Charpy impact test. Irradiation causes an increase in the DBTT and a decrease in USE. Steels have been developed that have excellent impact toughness and show relatively small changes in the properties under conditions where only displacement damage occurs. Under conditions were larger amounts of transmutation helium form, larger changes have been noted due to the intervention of intergranular fracture. The effects depend on temperature, and it may be possible to operate a spallation neutron target in temperature ranges to avoid the most severe problems. New low-DBTT steels offer some promise for greater resistance to radiation hardening related shifts in DBTT. Their resistance to intergranular failure at high helium concentrations needs to be determined. It may also be possible to develop low-chromium steels to reduce the helium effect.

## Acknowledgments

Research sponsored by the Office of Fusion Energy Sciences, U. S. Department of Energy, under contract DE-AC05-960R22464 with Lockheed Martin Energy Research Corp. Reviews of the manuscript by Drs. K. Farrell and D. J. Alexander are greatly appreciated.

## References

[1] S. N. Rosenwasser et al., J. Nucl. Mater., 85 & 86 (1979), 177.
[2] D. R. Harries, Proceedings of Topical Conference on Ferritic Steels for use in Nuclear Energy Technologies, ed. J. W. Davis and D. J. Michel (Warrendale, PA: The Metallurgical Society of AIME, 1984), 141.
[3] R. L. Klueh and E. E. Bloom, Nucl. Eng. Design/Fusion, 2 (1985), 383.
[4] D. S. Gelles, Optimizing Materials for Nuclear Applications, ed. F. A. Garner, D. S. Gelles, and F. W. Wiffen (Warrendale, PA: The Metallurgical Society, 1985), 63.
[5] D. Dulieu, K. W. Tupholme, and G. J. Butterworth, J. Nucl. Mater., 141-143 (1986), 1097.
[6] M. Tamura et al., J. Nucl. Mater., 141-143 (1986), 1067.
[7] E. E. Bloom, Radiation Damage in Metals, ed. N. L. Peterson and S. D. Harkness (Metals Park, OH: American Society for Metals, 1976), 295.
[8] R. L. Klueh and D. J. Alexander, J. Nucl. Mater., 187 (1992), 60.
[9] R. L. Klueh and D. J. Alexander, Effects of Radiation on Materials: 18th International Symposium, ASTM STP 1325, eds. R. K. Nanstad, M. L. Hamilton, F. A. Garner, and A. S. Kumar (Philadelphia: ASTM, 1997), to be published.
[10] D. S. Gelles, private communication with author, Pacific Northwest National Laboratory, 12 December 1996.
[11] D. S. Gelles, J. Nucl. Mater., 233-237 (1996), 293.
[12] D. S. Gelles and A. Kohyama, Fusion Reactor Materials Semiannual Progress Report for Period Ending March 31, 1989 (Report DOE/ER-0313/6, 1989), 193.
[13] D. S. Gelles, J. Nucl. Mater., 212-215 (1994), 714.
[14] J. M. Vitek and R. L. Klueh, Proceedings of Topical Conference on Ferritic Steels for use in Nuclear Energy Technologies, eds. J. W. Davis and D. J. Michel (Warrendale, PA: The Metallurgical Society of AIME, 1984), 551.
[15] R. L. Klueh and J. M. Vitek, J. Nucl. Mater., 132 (1985), 27.
[16] R. L. Klueh and J. M. Vitek, J. Nucl. Mater., 137 (1985), 44.
[17] R. L. Klueh and J. M. Vitek, J. Nucl. Mater., 182 (1991), 230.
[18] K. Farrell, Radiation Effects, 53 (1980), 175.
[19] R. L. Klueh and J. M. Vitek, J. Nucl. Mater., 161 (1989), 13.
[20] R. L. Klueh and J. M. Vitek, J. Nucl. Mater., 150 (1987), 272.
[21] R. L. Klueh and P. J. Maziasz, J. Nucl. Mater., 187 (1992), 43.
[22] D. Cramer, A. G. Pard, and C. G. Rhodes, Irradiation Embrittlement and Creep in Fuel Cladding and Core Components, (London: British Nuclear Energy Society, 1972), 109.
[23] C. Wassilew, Mechanical Behaviour And Nuclear Applications of Stainless Steel at Elevated Temperatures (London: The Metals Society, 1982), 172.
[24] R. L. Klueh, J. Nucl. Mater., 117 (1983), 295.
[25] J. R. Hawthorne, Treatise on Materials Science and Technology, Vol. 25 (New York: Academic Press, 1983), 461.
[26] R. L. Klueh and D. J. Alexander, Effects of Radiation on Materials: 15th International Symposium, ASTM STP 1125, ed. R. E. Stoller, A. S. Kumar, and D. S. Gelles (Philadelphia: ASTM, 1992), 1256.
[27] W. L. Hu and D. S. Gelles, Influence of Radiation on Material Properties: 13th International Symposium (Part II), ASTM STP 956, eds. F. A. Garner, C. H. Henager, Jr., and N. Igata, (Philadelphia: ASTM, 1987), 83-97.
[28] J. M. Vitek and R. L. Klueh, Met. Trans.A, 14A (1983) 1047.
[29] R. W. Hertzberg, Deformation and Fracture Mechanics of Engineering Materials, 3rd Edition (John Wiley & Sons, New York, 1989) p. 253.
[26] C. J. McMahon, Jr., Fundamental Phenomena in the Materials Sciences, Vol. 4, eds. L. J. Bonis, J. J. Duga, and J. J. Gilman, (Plenum Press, New York, 1967) p. 247.
[31] M. Rieth, B. Daffener, and H. D. Rohrig, J. Nucl. Mater., 233-237 (1996), 351.
[32] K. Ehrlich, private communication with author, KZK/Karlsruhe, 24 October 1996.
[33] R. L. Klueh and D. J. Alexander, J. Nucl. Mater., 187 (1992), 60.
[34] R. L. Klueh and D. J. Alexander, J. Nucl. Mater., 218 (1995), 151.
[35] W. R. Corwin, J. M. Vitek, and R. L. Klueh, J. Nucl. Mater., 149 (1987), 312.
[36] R. L. Klueh, J. M. Vitek, W. R. Corwin, and D. J. Alexander, J. Nucl. Mater., 155-157 (1988), 973.
[37] P. J. Maziasz and D. N. Braski, J. Nucl. Mater., 141-143 (1986), 973.
[38] R. L. Klueh, D. J. Alexander, and E. A. Kenik. J. Nucl. Mater., 227 (1995) 11.
[39] R. L. Klueh, D. J. Alexander, and P. J. Maziasz, Met. Trans. A, to be published.